QUADRATIC CONSTRAINED ENERGY MINIMIZATION FOR HYPERSPECTRAL TARGET DETECTION

*Zhengxia Zou, Zhenwei Shi**

Image Processing Center,
School of Astronautics, Beihang University,
Beijing 100191, P.R. China

Jun Wu, Hongqiang Wang

Remote Sensing and Mapping Department
Space Star Technology CO., Ltd.
Beijing 100086, P.R. China

ABSTRACT

In this paper, we propose a simple but effective algorithm, Quadratic Constrained Energy Minimization (QCEM) detector for hyperspectral image target detection. QCEM is a nonlinear version of classical Constrained Energy Minimization (CEM) detector, and it exploits the nonlinear characteristics of data by adding quadratic term on CEM model. Experimental results on one real hyperspectral images and one synthetic image suggest our method significantly improves the performance of the original CEM detection algorithm.

Index Terms— Hyperspectral image target detection, constrained energy minimization (CEM), Quadratic term, Regularization

1. INTRODUCTION

Hyperspectral imaging sensor collects digital images with very densely sampled radiance spectra in the scene. Among its wide range of applications, hyperspectral image target detection is one of the most important applications due to its both civil and military use. As each material is characterized by a unique deterministic spectrum, it is able to discriminate the materials based on the spectral characteristics. Several algorithms for hyperspectral target detection have been proposed in the past decades such as matched filter (MF) [1, 2], constrained energy minimization (CEM) [3], adaptive coherence estimator (ACE) [2, 4], adaptive matched filter (AMF) [5] and target-constrained interference-minimized filter (TCIMF) [6].

Among these methods, CEM algorithm imposes a constraint on the target spectrum, and simply build a linear filter detector which minimizes the output energy. However, distribution of the real hyperspectral data is complex. The uncompensated errors in the sensor, uncompensated atmospheric and variation in the material usually add nonlinearity to spectral data. Under these circumstances, linear filter detectors like CEM may obtain bad detection results. In this paper, we propose a simple but effective algorithm, Quadratic Constrained Energy Minimization (QCEM) detector for hyperspectral target detection. QCEM is a nonlinear version of classical CEM detector, and it exploits the nonlinear characteristics of data by adding quadratic term on CEM model. In order to enhance its robustness, a regularization term is further added. The contributions of our work are summarized as bellow:

1) We propose a novel hyperspectral target detection algorithm, QCEM.

2) We theoretically explained that why QCEM obtain a better detection performance than original CEM.

3) The proposed detector can be obtained by a closed-form formulation and is easy to implement.

2. A BRIEF INTRODUCTION TO CEM

Consider a hyperspectral image with N pixel vectors and L bands: $\mathbf{x}_i \in \mathbb{R}^{L\times 1}$, $i = 1, 2, \ldots, N$. All spectra of the N pixel hyperspectral image can be arranged in an $L \times N$ matrix as $\mathbf{X} = [\mathbf{x}_1, \mathbf{x}_2, \ldots, \mathbf{x}_N]$. The aim of CEM algorithm is to design an FIR filter specified by the vector $\mathbf{w} = [w_1, w_2, \ldots, w_L]^T$. The expectation of output energy can be represented as

$$E\{y^2\} = E\{(\mathbf{w}^T\mathbf{x})^2\} = \mathbf{w}^T E\{\mathbf{x}\mathbf{x}^T\}\mathbf{w} = \mathbf{w}^T\mathbf{R}\mathbf{w} \quad (1)$$

where $\mathbf{R} = E\{\mathbf{x}\mathbf{x}^T\}$ represents the correlation matrix. The CEM designs a FIR filter which minimizes the total output energy subject to a constraint that the filter's response to $\mathbf{d}$ is 1:

$$\begin{aligned} min\ \ & J(\mathbf{w}) = \mathbf{w}^T\mathbf{R}\mathbf{w} \\ s.t.\ \ & \mathbf{w}^T\mathbf{d} = 1 \end{aligned} \quad (2)$$

*Corresponding author. The work was supported by the National Natural Science Foundation of China under the Grants 61273245 and 91120301, the Beijing Natural Science Foundation under the Grant 4152031, the Program for New Century Excellent Talents in University of Ministry of Education of China under the Grant NCET-11-0775, the funding project of State Key Laboratory of Virtual Reality Technology and Systems, Beihang University under the Grant VR-2014-ZZ-02, and the Fundamental Research Funds for the Central Universities under the Grant YWF-14-YHXY-028, and the Open Research Fund of The Academy of Satellite Application under grant NO. 2014_CXJJ-YG_08.

where $\mathbf{d}$ is the target spectrum and can be obtained by averaging different target spectral vectors of a certain material in one hyperspectral image. The solution of the above optimization problem is given by [3] which is

$$\mathbf{w}^* = \frac{\mathbf{R}^{-1}\mathbf{d}}{\mathbf{d}^T\mathbf{R}^{-1}\mathbf{d}}. \tag{3}$$

Thus the output of the CEM filter for a test pixel $\mathbf{x}_i$ is given by

$$y_i = (\mathbf{w}^*)^T\mathbf{x}_i = \frac{\mathbf{d}^T\mathbf{R}^{-1}}{\mathbf{d}\mathbf{R}^{-1}\mathbf{d}^T}\mathbf{x}_i. \tag{4}$$

3. QUADRATIC CONSTRAINED ENERGY MINIMIZATION DETECTOR

QCEM algorithm aims to design an nonlinear filter specified by a diagnosed matrix $\mathbf{G} = diag(g_1, g_2, \ldots, g_L)$ and a vector $\mathbf{w} = [w_1, w_2, \ldots, w_L]^T$. For a test pixel $\mathbf{x}_i \in \mathbb{R}^{L\times 1}$, output of QCEM filter can be expressed by the following quadratic filter

$$y_i = \mathbf{x}_i^T\mathbf{G}\mathbf{x}_i + \mathbf{w}^T\mathbf{x}_i. \tag{5}$$

In QCEM algorithm, $\mathbf{w}$ and $\mathbf{G}$ can be determined by the following optimization problem

$$\begin{aligned} &min\ \ J(\mathbf{w},\mathbf{G}) = E\{y^2\} + \beta(\|\mathbf{w}\|_F^2 + \|\mathbf{G}\|_F^2) \\ &s.t.\ \ \mathbf{d}^T\mathbf{G}\mathbf{d} + \mathbf{w}^T\mathbf{d} = 1, \end{aligned} \tag{6}$$

where $\|\cdot\|_F$ represents the Frobenius norm of a matrix and β is a positive number which is used to control the amount of regularization. In (6), the objective function $J(\mathbf{w},\mathbf{G})$ consists of two parts. The first part $E\{y^2\}$ represents the expectation of output energy. The second part $\beta(\|\mathbf{w}\|_F^2 + \|\mathbf{G}\|_F^2)$ is a regularization termwhich aims to reduce the complexity of the filter and increase its stability. QCEM aims to design a nonlinear filter detector, which minimizes the output energy and the regularization term at the same time, meanwhile, the filter's response to the target spectrum $\mathbf{d}$ is subjected to 1. In order to solve this matrix optimization problem, the objective function $J(\mathbf{w},\mathbf{G})$ can be expanded as

$$\begin{aligned} J(\mathbf{w},\mathbf{G}) &= E\{(\mathbf{x}^T\mathbf{G}\mathbf{x} + \mathbf{w}^T\mathbf{x})^2\} + \beta(\|\mathbf{w}\|_F^2 + \|\mathbf{G}\|_F^2) \\ &= E\{(\sum_{j=i}^{L} w_j x_j + \sum_{j=i}^{L} g_j x_j^2)^2\} + \beta\sum_{j=1}^{L}(w_j^2 + g_j^2) \\ &= E\{(\mathbf{r}^T\tilde{\mathbf{x}})^2\} + \beta\|\mathbf{r}\|_2^2, \end{aligned} \tag{7}$$

where

$$\begin{aligned} \mathbf{r} &= [w_1, w_2, \ldots, w_L, g_1, g_2, \ldots, g_L]^T \in \mathbb{R}^{2L\times 1}, \\ \tilde{\mathbf{x}} &= [x_1, x_2, \ldots, x_L, x_1^2, x_2^2, \ldots, x_L^2]^T \in \mathbb{R}^{2L\times 1} \end{aligned} \tag{8}$$

represent the expanded coefficient vector and the expanded spectral data, respectively. Similarly, the constrain term of (6) also can be expanded as

$$\mathbf{d}^T\mathbf{G}\mathbf{d} + \mathbf{w}^T\mathbf{d} = \sum_{j=1}^{L} w_j d_j + \sum_{j=1}^{L} g_j d_j^2 = \mathbf{r}^T\tilde{\mathbf{d}}, \tag{9}$$

where

$$\tilde{\mathbf{d}} = [d_1, d_2, \ldots, d_L, d_1^2, d_2^2, \ldots, d_L^2]^T \in \mathbb{R}^{2L\times 1} \tag{10}$$

represents the expanded target spectral data. Thus, by using the transformation (8) and (10), the matrix optimization problem (6) can be transformed into the following vector optimization problem

$$\begin{aligned} &min\ \ J(\mathbf{r}) = E\{(\mathbf{r}^T\tilde{\mathbf{x}}\} + \beta(\|\mathbf{r}\|_2^2) \\ &s.t.\ \ \mathbf{r}^T\tilde{\mathbf{d}} = 1. \end{aligned} \tag{11}$$

The problem (11) can be easily solved, and have the following closed-form solution

$$\mathbf{r}^* = \frac{(E\{\tilde{\mathbf{x}}\tilde{\mathbf{x}}^T\} + \beta\mathbf{I})^{-1}\tilde{\mathbf{d}}}{\tilde{\mathbf{d}}^T(E\{\tilde{\mathbf{x}}\tilde{\mathbf{x}}^T\} + \beta\mathbf{I})^{-1}\tilde{\mathbf{d}}}. \tag{12}$$

Thus the output of the QCEM filter for a test pixel $\mathbf{x}_i$ can be obtained by

$$y_i = \mathbf{x}_i^T\mathbf{G}^*\mathbf{x}_i + \mathbf{w}^{*T}\mathbf{x}_i = \mathbf{r}^{*T}\tilde{\mathbf{x}}_i. \tag{13}$$

4. EXPERIMENT ON SYNTHETIC HYPERSPECTRAL DATA

The spectral library we used in this experiment is provided by the United States Geological Survey (USGS) [7] digital spectral library. 15 endmember signatures are used to generate our synthetic data, including Labradorite HS17.3B, Rhodochrosite HS67, etc. The above 15 spectra are collected in 224 bands uniformly spanning from 0.4 to 2.5 μm. In this experiment, Labradorite HS17.3B is used as the target spectrum. We used the target implantation method introduced by Chang et al. [8] to generate the synthetic data. We first divide the synthetic map, whose size is $s^2 \times s^2$ (s = 8), into $s \times s$ regions. Each region is initialized with the same type of ground cover which is randomly selected from the above 15 kinds of signatures. Then mix the synthetic map through a $(s+1) \times (s+1)$ spatial low-pass filter. Finally we implant clean target into the backgrounds by replacing their corresponding pixels. In order to evaluate the detector's variability, both targets and backgrounds are corrupted by a Gaussian white noise with 30 dB SNR at the same time. Fig. 1(a) shows the first band of the synthetic image and Fig. 1(b) shows the groundtruth.

The regularization parameter β of our QCEM algorithm is set to 0.01. In this experiment, we compare our QCEM with the original CEM algorithm [3]. In order to further evaluate the effect of the quadratic term in (5), we also compare with

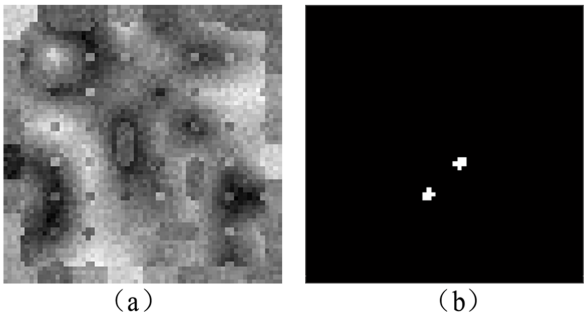

Fig. 1. (a) First band of the synthetic hyperspectral image. (b) Truth distribution of the targets (groundtruth).

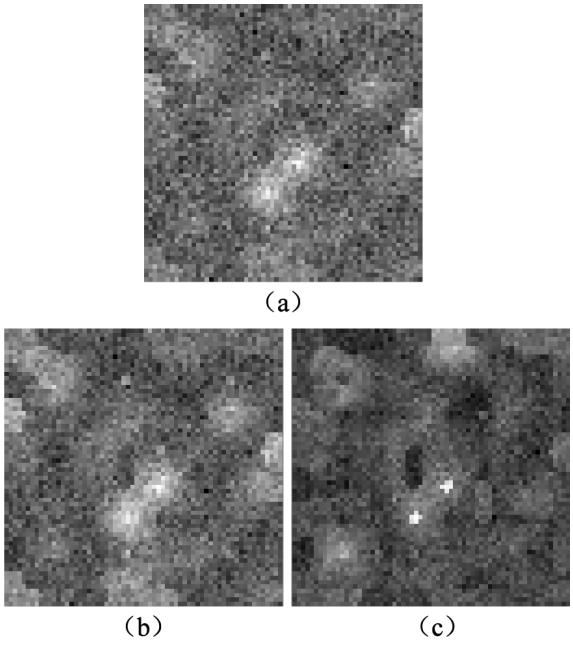

Fig. 2. Detection results of (a) CEM algorithm, (b) regularization-CEM algorithm and (c) our QCEM algorithm on synthetic data.

regularization-CEM algorithm (QCEM without quadratic term). Fig. 2 shows the outputs of the (a) original CEM, (b) regularization-CEM and (c) the proposed QCEM. Outputs of all detectors in Fig. 2 are normalized to [0,1] for comparison. From Fig. 2 we can see the highest detection score of the targets by the our QCEM algorithm generally correspond with those pixels belong to the groundtruth image. The result suggests that our algorithm outperforms the other two algorithms.

To further illustrate the effectiveness of our hierarchical architecture, the Receiver Operating Characteristics (ROC) [9] curves are used. The ROC curves describe the varying relationship of detection probability and false alarm rate, and provide performance comparison of the different detectors [4, 9]. Based on the groundtruth image, the ROC curve gives the relationship between the false alarm rate (Fa) and the probability of detection (Pd) by changing different thresholds on a detector's output. Fa and Pd are defined as follows:

$$Fa = \frac{N_f}{N_b}, \quad Pd = \frac{N_c}{N_t}, \tag{14}$$

where N_f is the number of false alarm pixels, N_b is the total number of background pixels, N_c is the number of correct detection target pixels and N_t is the number of total true target pixels. Fig. 3 shows the ROC curves of the above three detection algorithms. Our QCEM algorithm has significantly enhanced the performance of the original CEM algorithm and get the best detection result.

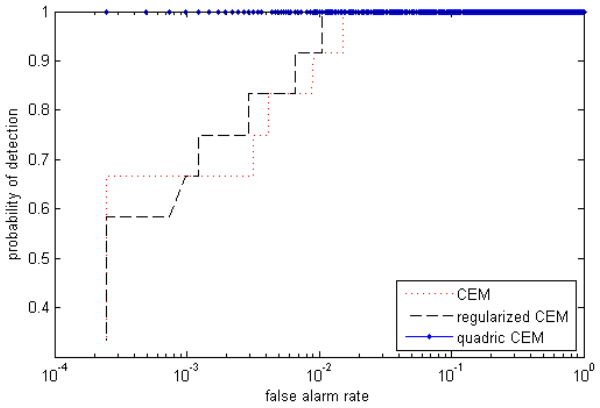

Fig. 3. The ROC curves on the synthetic hyperspectral image.

5. EXPERIMENT ON REAL HYPERSPECTRAL DATA

A real hyperspectral image is also used to conducted the experiment. The data is a part of the airport in San Diego, America, and is collected by the Airborne Visible/InfraRed Imaging Spectrometer (AVIRIS). The AVIRIS sensor collects the spectral data in 224 bands spanning from 0.4 to 2.5 μm. The size of each band is 200×200 pixels. The first band of the hyperspectral image is shown in Fig. 4(a) and Fig. 4(b) shows the groundtruth. We can see that three airplanes are located in the left half of the image. The target spectrum $\mathbf{d}$ used in this experiment is provided by the spectral library on the Internet. The regularization parameter β of our QCEM algorithm is set to 0.01, which is the same as it was used in the last experiment. Fig. 5 shows the detection results: (a) original CEM, (b) regularized-CEM and (c) the proposed QCEM. Fig. 6 shows the ROC curves of three above mentioned methods' detection results. The ROC curves further prove that our algorithm largely improve the original CEM and regularized-CEM algorithm on real hyperspectral data.

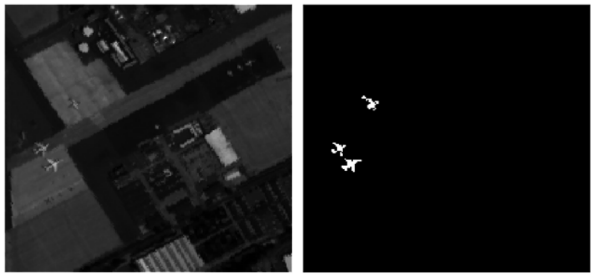

(a) (b)

Fig. 4. (a) First band of the AVIRIS image. (b) Truth distribution of the targets (groundtruth).

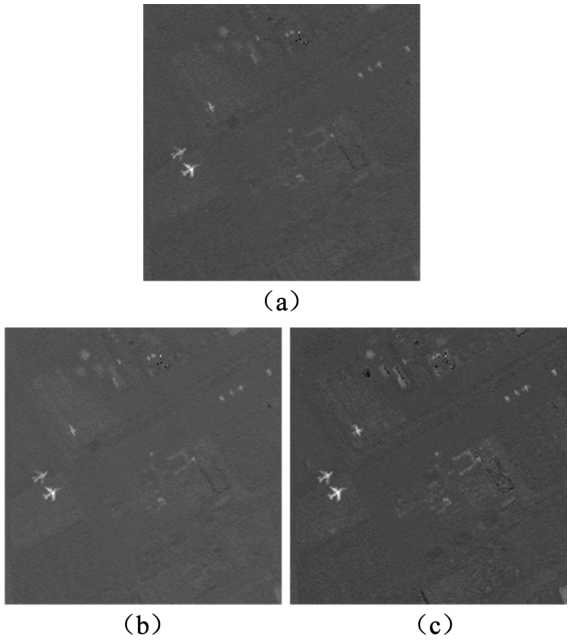

(a)

(b) (c)

Fig. 5. Detection results of (a) CEM algorithm, (b) regularized-CEM algorithm and (c) our QCEM algorithm on AVIRIS data.

6. CONCLUSION

In this paper, we propose a new hyperspectral target detection algorithm, Quadratic Constrained Energy Minimization (QCEM) algorithm. QCEM is a nonlinear version of original CEM algorithm. Experimental results on one real hyperspectral image and one synthetic hyperspectral image suggest that QCEM has significantly improved the performance of original CEM.

7. REFERENCES

[1] S. M. Kay, "Fundamentals of Statistical Signal Processing: Detection Theory, vol. 2," *Prentice Hall Upper Saddle River, NJ, USA:*, 1998.

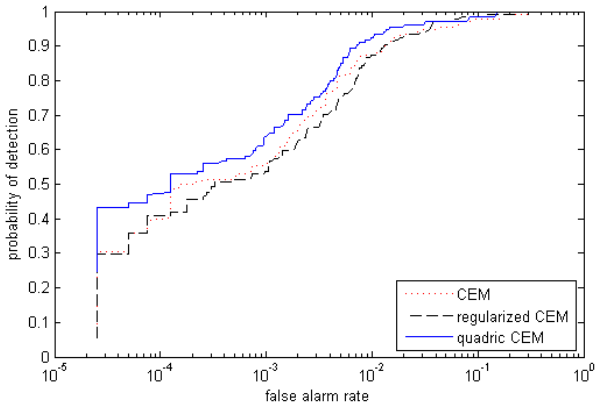

Fig. 6. The ROC curves on the AVIRIS hyperspectral image.

[2] D. G. Manolakis, R. Lockwood, T. Cooley and J. Jacobson, "Is there a best hyperspectral detection algorithm?" *SPIE Defense, Security, and Sensing*, vol. 7334, 733402, 2009.

[3] W. H. Farrand, and J. C. Harsanyi, "Mapping the distribution of mine tailings in the Coeur d'Alene River Valley, Idaho, through the use of a constrained energy minimization technique," *Remote Sensing of Environment*, vol. 59, pp. 64-76, 1997.

[4] D. G. Manolakis, D. Marden and G. A. Shaw, "Hyperspectral image processing for automatic target detection applications," *Lincoln Laboratory Journal*, vol. 14, no. 1, pp. 79-116, 2003.

[5] F. C. Robey, D. R. Fuhrmann, E. J. Kelly, and R. Nitzberg, "A CFAR adaptive matched filter detector," *IEEE Trans. Aerosp. Electron. Syst.*, vol. 28, no. 1, pp. 208-216, 1992.

[6] H. Ren and C.-I. Chang, "Target-constrained interference-minimized approach to subpixel target detection for hyperspectral images," *Opt. Eng.*, vol. 39, pp. 3138-3145, 2000.

[7] R. Clark, G. Swayze, A. Gallagher, T. King and W. Calvin, "The US Geological Survey digital spectral library: Version 1 (0.2 to 3.0 μm), Open File Report 93-592" *US Geological Survey*, 1993.

[8] Y. C. Chang, H. Ren, C. I. Chang, and R. S. Rand, "How to design synthetic images to validate and evaluate hyperspectral imaging algorithms," *SPIE Defense and Security Symposium*, vol. 6966, 69661P, 2008.

[9] C. Chang , "Multiparameter receiver operating characteristic analysis for signal detection and classification," *Sensors Journal, IEEE*, vol. 10, no. 3, pp. 423-442, 2010.